# Accepted Manuscript

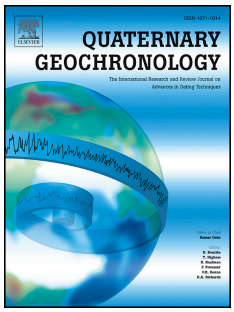


Exploring the dating of “dirty” speleothems and cave sinters using radiocarbon dating of preserved organic matter

Alison J. Blyth, Quan Hua, Andrew Smith, Silvia Frisia, Andrea Borsato, John Hellstrom

PII: S1871-1014(16)30053-X

DOI: 10.1016/j.quageo.2017.02.002

Reference: QUAGEO 823

To appear in: *Quaternary Geochronology*

Received Date: 23 May 2016

Revised Date: 10 October 2016

Accepted Date: 6 February 2017

Please cite this article as: Blyth, A.J., Hua, Q., Smith, A., Frisia, S., Borsato, A., Hellstrom, J., Exploring the dating of “dirty” speleothems and cave sinters using radiocarbon dating of preserved organic matter, *Quaternary Geochronology* (2017), doi: 10.1016/j.quageo.2017.02.002.

# Exploring the dating of "dirty" speleothems and cave sinters using radiocarbon dating of preserved organic matter

Alison J Blyth[a*], Quan Hua[b], Andrew Smith[b], Silvia Frisia[c], Andrea Borsato[c], John Hellstrom[d]

[a]The Institute of Geoscience Research and the Western Australian School of Mines, Curtin University, GPO Box U1987, Perth 6845, Western Australia, Australia

[b]Australian Nuclear Science and Technology Organisation, Locked Bag 2001, Kirrawee DC, NSW 2232, Australia

[c]School of Environmental and Life Sciences, The University of Newcastle, NSW 2308 Australia

[d]School of Earth Sciences, The University of Melbourne, VIC 3010 Australia

*corresponding author, email alison.blyth@curtin.edu.au; phone +61 8 9266 9388

**Abstract**

Speleothems and other carbonate deposits such as tufa containing high proportions of detrital material can be difficult to chemically date due to detrital thorium levels causing a high level of error in conventional U-Th disequilibrium dating. Here we investigate the use of an alternative technique centring on radiocarbon dating of organic matter preserved within the detrital fraction. Non-acid soluble humic, particulate and detritally absorbed organic matter was recovered from eight samples from a flowstone sinter formed within a roman aqueduct at Trento in Italy with a maximum age of 100 CE (1850 cal yr BP), and two repeat samples from a dripstone formed within the 20$^{th}$ Century on a wire fence at Lilly-Pilly Cave, Buchan Caves Reserve in Victoria, Australia. In the aqueduct samples the median calibrated $^{14}$C ages ranged from 2232 to 2889 cal yr BP, with 95.4% probability age range in the youngest and oldest samples of 2153 - 2337 and 2342 – 3449 cal yr BP respectively. The median age of the more modern dripstone was 336 cal yr BP, with a 95.4% probability age range of 148 to 486 cal yr BP. These results provide very approximate ball-park estimates of the age of the sample, but are consistently too old when compared to the known maximum ages of formation. It is hypothesised that this offset is due to a combination of the nature of the organic carbon transported from the source organic matter pools, and reworking of both modern and old organic carbon by in situ microbial communities.

**Keywords**

Speleothems; carbonate sinter; dating; radiocarbon; organic matter;

## 1. Introduction

One of the strengths in the use of carbonates such as speleothems as palaeoclimatic archives lies in their amenability to precise dating. The carbonate in speleothems is most frequently dated by uranium - thorium disequilibrium series (U-Th), which works well back to 500 ka (Dorale and Richards 2003; Dorale et al., 2004; Hellstrom et al., 2006; Hellstrom & Pickering 2015). Uranium – lead dating (U-Pb) extended our capability of obtaining ages from terrestrial carbonates well beyond this, from 1 Ma to at least 8 Ma (Woodhead et al., 2006). Radiocarbon has been relatively under-used as a dating technique in speleothems, principally because radiocarbon dating of the calcite requires corrections for issues such as the dead carbon proportion (dcp), meaning that most of the studies to date have focused on younger material where detection of the bomb spike allows for more accurate modelling (Genty & Massault 1997; Blyth et al., 2007; Hodge et al., 2011; Hua et al., 2012). Radiocarbon analysis in older speleothems has been focused on samples where the analyses could be paired with high precision U-Th dating for radiocarbon calibration (e.g. Beck et al., 2001; Hoffman et al., 2010; Southon et al., 2012) and investigation of temporal dcp variations (e.g., Rudzka et al., 2011; Griffiths et al., 2012; Noronha et al., 2014). These analyses of radiocarbon in speleothems have focused on the carbonate component derived from dissolved carbon dioxide from the breakdown of soil and vadose zone organic matter, and/or from dissolved calcium carbonate bedrock (Genty & Massault, 1999; Genty et al., 2001; Hua et al., 2012).

"Dirty" carbonates, those with significant detrital components incorporated in the matrix, are problematic from a dating point of view, as the detrital content has a tendency to lead to high detrital thorium levels which affects conventional chemical dating (Labonne

et al., 2002; Hellstrom 2006; Hua et al., 2012; Meyer et al., 2012). Although many samples are amenable to correction (e.g. Hellstrom 2006), and others allow for radiocarbon dating of the carbonate (e.g. Labonne et al., 2002), for some, it can become impossible to secure a usable dating frame-work. This effectively renders these samples defunct for many forms of palaeoenvironmental work, leading to the collected material being under-studied (Meyer et al., 2012). However, "dirty" material often also contains a relatively high organic content (Blyth et al., 2008; Blyth et al., 2015), thus opening up the possibility of using radiocarbon dating of the preserved organic matter as a partial solution to this problem. To date, we are aware of only limited radiocarbon studies that utilised the organic matter preserved in speleothems, probably because the proportion of TOC has been historically hard to measure in this context and is generally very low (0.01 – 0.3% of total carbon; Blyth et al., 2013; Li et al., 2014; Quiers et al. 2015; Blyth et al., 2016). However, radiocarbon dating of organic compounds in moonmilk flowstones from high alpine settings, consisting of fibrous calcite crystals and with a large organic matter component (Borsato et al., 2000; Blyth & Frisia, 2008), have yielded ages consistent with those of crystalline speleothems at lower altitudes in the same area, which allowed reconstruction of long-term Holocene climate (Frisia & Borsato, 2010). Radiocarbon dating on calcareous tufa flowstones from the same alpine region, which consist of a mixture of biomediated calcite crystals, detrital components and organic matter, yielded similar ages, although inversions were common (Borsato et al., 2007). Separately, dates from Lascaux cave in France have been published, based on calcite gours, which were observed to have a mineral structure reminiscent of moonmilk (Genty et al., 2011). Four organic matter dates were obtained from this material, based on organic residue that was observed to have a filamentous structure similar to that from fungal and algal remains found in carbonate tufas (Genty et al., 2011). These dates were found to be

older by approximately 500 years than those from charcoal from comparable layers, and to have a disturbed chronology (Genty et al., 2011). These results suggest that "dirty" conventional speleothems (such as stalagmites and flowstones) known to contain organic matter could potentially be dated with the radiocarbon method, but that sources and chronological disturbances need careful consideration. In this study we consider two different speleothem types from very different contexts to assess whether the issue of radiocarbon dating of organic matter returning older than expected ages is likely to be a widespread problem, or site-specific.

## 2. Materials and methods

### *2.1 Samples*

The principal sample in this study is a flowstone sinter formed inside a roman aqueduct at Trento in the Italian Dolomites (henceforth referred to by the sample code T-AQ). The use of a sample from a man-made structure allows us to place a maximum date of formation independent of any chemical techniques, in this case of circa 100 CE, or 1850 cal yr BP, the aqueduct being believed to have been built during the last quarter of the 1$^{st}$ century (75-100 CE) and utilised until the fall of the Roman Empire and the Early Middle Ages, around 500 CE (Bassi, 2004, 2007). The sample is taken from a section of the aqueduct that was unearthed in the late 1990s, with studies suggesting the water was sourced from groundwater draining Permian to Mesozoic carbonate-evaporite-siliciclastic rocks (Bassi, 2004). That the waters feeding the aqueduct were captured from karst springs, rather than surface waters, is supported by the mineral fabrics of the flowstone and $\delta^{13}C$ data, which

110 are typical for stalagmites/flowstones grown in caves at mid-altitudes, below the conifer
111 vegetation belt in the region (Frisia & Borsato 2010; Borsato et al., 2015)

112 The flowstone, or sinter, which has grown upon a cement mortar layer, is about 400
113 mm wide and up to 105 mm thick. The most common facies is characterized by lamina
114 couplets marked by differences in porosity and fabric, with variations in the percentage of
115 sparite and micrite. The columnar fabric (Frisia, 2015) consists of fans of sparry calcite
116 crystals, commonly showing rounded crystal terminations capped by micrite laminae. Spar
117 crystals may be partially truncated by micrite, show fine impurity-rich lines, and split into
118 crystals arranged in fans (Fig. 1). Crystal tips can be corroded, as documented also in
119 stalagmitic flowstones. Micrite is arranged in laminae capping the spar crystals, and is
120 commonly aggregated in peloids (Frisia, 2015) associated with Fe-oxides, silt and small
121 bivalves (Fig 1.). Both micrite and sparite consist of low-Mg calcite with variable amounts of
122 detrital fraction, mostly associated with the micrite, including quartz, feldspar, dolomite,
123 gypsum, particulate organic matter, clay minerals. EDXS analyses identified the presence of
124 P, up to 5%, in the micrite layers, which is most likely to be associated with dead microbial
125 matter and, possibly, allogenic bone fragments. The micrite layers show fluorescence when
126 excited by blue light at 365 nm, whereas the sparry calcite show fluorescence when excited
127 by both green (470 nm) and blue light. This may be indicative of the presence, in both the
128 micrite and sparite, of the by-products of organic matter degradation.

129 The T-AQ sinter grew in an artificial tunnel, with a higher discharge (in the order of 5
130 to 20 l/sec) than that commonly observed for cave flowstones. However, as the aqueduct
131 was capped by stone slabs, most of the microflora and fauna living within the structure
132 would be adapted to a dark environment. As is the case for cave speleothems (Blyth et al.,
133 2008; Blyth et al., 2016), the sinter's organic content is likely to reflect a mixture of

transported particles and solutes and locally produced organic compounds. The T-AQ sinter can therefore be taken as an analogue for those flowstones and rimstone dams (cave calcareous tufa) which developed in periods of relatively fast flow, in a context amenable to microbial growth.

Radiocarbon analyses were performed on eight subsamples collected from the flowstone in a consecutive sequence from top to base (Fig 2.), each weighing between 8 and 12 g dry calcite. Repeat calcite subsamples were processed and analysed for levels 2, 3, 5, 6, and 7 to provide better dating control. Subsections were cut using a diamond wire saw, and only clean water as lubricant. After air drying, samples were stored in aluminium foil.

To test the method in a more conventional speleothem, two samples of 5 g of dry calcite each were analysed from a dripstone (LP-13) grown in Lilly-Pilly Cave, Buchan Caves Reserve, Murrindal, Victoria, Australia. This dripstone sample formed on a wire fence within the cave, thus enabling an external control to limit its time of formation to the 20th century. The LP-13 calcite contains reddish brown dirt visible by eye, which is commonly seen in speleothems at this site, and is believed to result from flushes of detrital material during periods of high flux (Nicholas White, pers comm.). The dripstone was sampled directly into annealed glass containers to minimise contamination and any exposure to fingerprints or plastic.

*2.2 Uranium-thorium dating*

The T-AQ material forms a challenge for U-Th dating because of its high porosity and visible interspersed detritus, but U-Th analysis was attempted to provide a context for the radiocarbon and to test whether the sample has behaved as a closed system for U. Samples

158 were drilled from the top and base of the specimen (layers 1 and 8 respectively). ~25 mg
159 subsamples were dissolved and spiked with a mixed $^{229}$Th-$^{233}$U-$^{236}$U tracer followed by
160 extraction of the actinide fraction using Eichrom TRU resin. U and Th isotope ratios were
161 measured simultaneously using a Nu Plasma multi-collector ICP mass spectrometer at the
162 University of Melbourne (Hellstrom, 2003; Drysdale et al, 2012).
163
164 *2.3 Extraction method for radiocarbon dating*
165
166 The aim of the extraction method was to maximise recovery of the particulate
167 organic matter present in the speleothems along with as much of the non-acid soluble
168 organic matter as possible, whilst also removing any acid salts that would interfere with safe
169 combustion, minimising contamination levels from exposure to reagents and equipment,
170 and delivering a method that could be undertaken in a standard laboratory within a
171 reasonable time-frame, and be adaptable to a range of carbonates. Early experiments with
172 recovery of organics via filtering the sample were not suited to speleothems without
173 significant clay detritus, as effective recovery of organic matter from the filter proved
174 problematic, and the technique exposed the samples to increased potential contamination
175 sources. A method based on centrifuge recovery was therefore chosen.
176 The solid sectioned speleothem subsamples were cleaned in 3 M HCl (Sigma-Aldrich,
177 ACS grade, in glass) to remove surface contamination, and then washed sequentially in
178 MilliQ water, and by sonication (x 10 mins) in methanol, and then dichloromethane (DCM)
179 to wash out the surface pores of the calcite. The cleaned sections were digested in 3 M HCl
180 in 50 ml pyrex centrifuge tubes which had been pre-annealed at 450 °C. The minimum
181 amount of acid required for full digestion was used; as per Blyth et al. (2006), the acid was

cleaned prior to use via liquid-liquid extraction in DCM. Once digestion was complete, the solution was settled, and as much supernatant as possible was removed with a pre-annealed glass pipette without disturbing the particulate sediment. The top of the pipette was plugged with a loose small wad of cleaned glass wool to prevent any contamination being transferred from the pipette bulb.

MilliQ water was added to the sample tubes to remove acid salts, and the tubes centrifuged at 1500 rpm for 10 mins to settle the maximum amount of organic sediment, before excess wash water was removed with a pipette. For this material, two washes of 40 ml MilliQ water each were found to be adequate. The particulate sediment in each tube was taken up in the last 2 ml of water from the final wash, and transferred to pre-weighed annealed 4 ml vials, the residue was oven-dried at 80-100 °C and weighed. This step is only necessary in samples like these where the physical amount of particulate matter is too large to be suitable for direct transfer to the quartz combustion tube. After weighing, an aliquot of the residue equivalent to 2 – 12 mg dry weight (n.b. this refers to complete dry residue including clay, not carbon content) was transferred in 0.5 ml of MilliQ water to pre-annealed wide bore quartz tubes (6 mm OD x 120 mm), and oven-dried at 100 °C. Quartz tubes were capped with cleaned foil and lab film for transfer from Curtin University to the Australian Nuclear Science and Technology Organisation (ANSTO) for radiocarbon analysis.

At ANSTO, the quartz tubes containing sample sediment were combusted and the resultant sample $CO_2$ was converted to graphite following standard procedures (Hua et al., 2001). The graphite was loaded into an aluminium cathode by rear pressing for $^{14}C$ analysis using the ANTARES accelerator mass spectrometry (AMS) facility at ANSTO (Fink et al., 2004).

206 **2.4 Preparation of procedural blanks**

207

208 To estimate the level of carbon contamination or extraneous carbon incorporated
209 during the full process of sample preparation including particulate extraction and AMS
210 procedure, two series of full procedural blanks at various carbon masses were prepared.
211 Blanks followed the full cleaning and extraction procedure using empty glassware, and were
212 spiked at the end of the process with either spectroscopic grade powdered graphite (Lot No.
213 40V) from Union Carbide containing no measurable $^{14}C$ or lignin alkali powder (Sigma-
214 Aldrich CAS 8068-06-1) having a $^{14}C$ level of ~125 percent Modern Carbon (pMC). This
215 determination of the $^{14}C$ content and mass of extraneous carbon is necessary for a proper
216 blank correction for the measured $^{14}C$ ages of our particulate samples.

217

218 **3. Results and discussion**

219

220 *3.1 U-Th dating*

221

222 Table 1 shows the U-Th data for the base (B) and top (T) of the T-AQ sinter. The
223 known historical age range of the flowstone constrains the initial $^{230}Th/^{232}Th$ activity ratio to
224 between 0.88 and 0.99, and Th-corrected U-Th ages were calculated using an average value
225 of 0.94 with an uncertainty of 5%. The resulting ages are inverted, but within the
226 uncertainty resulting from initial $^{230}Th/^{232}Th$ variability. There is no clear indication of post-
227 depositional diagenetic change, and the results can be explained entirely in terms of closed-
228 system evolution from a reasonable initial $^{230}Th/^{232}Th$ value.

229

*3.2 Radiocarbon*

All the T-AQ and LP samples were of sufficient size to allow radiocarbon dating, with carbon masses ranging from 0.06 – 0.19 mgC per sample. The measured $^{14}C$ values of these 15 samples in pMC are shown in Table 2.

The 21 procedural blanks (11 spiked with powdered graphite and 10 with lignin alkali) had carbon masses ranging from 0.045 to 0.96 mgC. Their pMC values presented in Fig. 3 show clear mass-dependent trends following hyperbolic curves very well, indicating that a constant level of carbon contamination was incorporated during our sample processing (Donahue et al., 1990). Using the method described by Hua et al. (2004), we have determined the $^{14}C$ content and mass of extraneous carbon incorporated during our sample processing. These values are 20.72 ± 3.09 pMC and 4.13 ± 0.43 µgC, respectively. We have used these values for blank correction for all measured samples using a two component mixing model (Brown and Southon, 1997; Hua et al., 2004), and the corrected $^{14}C$ ages of all particulate samples are also presented in Table 2. Radiocarbon ages were converted to calendar ages using OxCal Program v.4.2 (Bronk Ramsey, 2009), and the SHCal13 data set (Hogg et al., 2013) for LP samples or the IntCal13 data set (Reimer et al., 2013) for T-AQ samples. Where replicate speleothem samples have been analysed, the $^{14}C$ ages agree with each other within 1σ uncertainties. The only exceptions to this are the samples from T-AQ-7, whose ages do not agree within 2σ uncertainties. This greater level of variation in one sample is likely to derive from a particularly high degree of mixed and reworked detrital material in this layer (Fig 2.).

All the calibrated $^{14}C$ ages of particulate samples from both LP-13 and T-AQ are consistently older than their known maximum age of formation by around 300 years for LP-13, and 300 – 1000 years for T-AQ (300 – 700 years, excluding T-AQ-7r, Fig 4.). This is consistent with the 500 year offset found by Genty et al. (2011). The middle samples from T-AQ (layers 2 – 6) also all have very similar dates within error of each other. We hypothesise that the consistent older dates of these samples are due to substantially older organic carbon being transported from the source organic matter pools with slow turnover times, combined with recycling of dead carbon by microbes within the aquifer. A recent study of a karst soil showed that the radiocarbon age of the bulk particulate organic matter spans from modern to over 2000 years BP (Hobley et al., 2014). As leaching from soil organic pools is assumed to be a major source for organic matter in karst groundwaters (Baker et al., 1999), it would be consistent for a similar mixture to be seen in speleothems (Blyth et al., 2008).

In the T-AQ samples, the fabrics support this interpretation. The columnar and micrite fabrics observed in T-AQ are commonly observed in other roman aqueduct carbonate sinters (Adolphe, 1973; Guendon & Vaudour, 1986), modern freshwater tufas (Gradzinski, 2010; Frisia & Borsato, 2010), cave flowstones and in some stalagmites (Frisia et al., 2000; Frisia & Borsato, 2010; Frisia, 2015). Similar features described in freshwater laminar tufa carbonates have been interpreted as primary depositional fabrics (Brasier et al., 2011) related to seasonal fluctuations in discharge (Arenas et al., 2010; Brasier et al., 2011) and, subsequently, in particulate content and water supersaturation with respect to calcite (Genty, 1992). Sparry columnar crystal development has been related to high-energy (discharge) periods in tufa (Gradziński, 2010) and to relatively constant drip rate in stalagmites (Frisia, 2015), which prevents colonization by micro-organisms, whilst micrite has been observed to form in low-energy periods (Gradziński, 2010) or under low drip rates

277 (Frisia & Borsato, 2010; Frisia, 2015). As documented for Holocene stalagmites from the
278 same region, organic-rich layers mark autumnal rains and flushing of soil organic
279 compounds and colloidal particulates (Frisia et al., 2000; Scholz et al., 2012). In T-AQ, thus,
280 we interpret fabrics as being mainly controlled by discharge.

281 The presence of peloidal micrite associated with Fe oxides arranged in stromatolite-
282 like layers in the T-AQ specimen suggests the presence of iron oxidising bacteria, similar to
283 *Leptotrhrix ochracea*, which grow in freshwater environments in periods of low discharge
284 (Pelczar et al., 1982). Thus, the formation of micrite should mark a combination of relatively
285 low flow and a higher abundance of particulate matter (cf. Arenas et al., 2010). Micritic
286 fabrics in freshwater tufa have been linked to the presence of Extra Polymeric Substances
287 (EPS) produced by microbes, which are believed to provide nucleation sites for calcite
288 (Rogerson et al., 2008). It is thus reasonable to infer that low discharge promoted growth of
289 microbial mats or filaments, which trapped and incorporated organic and detrital particles.
290 Small freshwater bivalves appear to have also been part of the community dwelling on the
291 aqueduct floor during low discharge periods. Radiocarbon ages of spring tufas show that the
292 "authochthonous" organic compounds (i.e. those generated in situ by microbial activity)
293 included in the deposit inherit their C from a mixture of atmospheric $CO_2$, biogenic old C and
294 old dissolved carbonates (Özkul et al., 2010). Similarly, in the Roman aqueduct, organic
295 compounds generated by the activity of microorganisms at the interface between substrate
296 and water may have resulted in the incorporation in the sinter of old C from dissolved
297 carbonate rocks, particulates or shells. Old C can also be associated with trapped particles
298 such as charcoal, bones or soil micro aggregates, which are known to retain soil organic
299 carbon (Hobley et al., 2013) and are to be expected in waters captured from a natural spring
300 or stream. Thus, both the transported and in situ organic matter deposited in T-AQ would

be expected to contain a mixture of older carbon and contemporaneous terrestrial carbon, as is seen in tufa. A similar argument can be made for the cave dripstone deposit LP-13, which contained visible amounts of transported detritus, but also contains glycerol dialkyl glycerol tetraethers (Blyth, unpublished data), which have been argued in speleothems to be principally derived from microbial populations living in-situ in the cave environment (Blyth et al., 2014; Baker et al., 2016).

## 4. Potential for future application

The results from this experiment suggest that radiocarbon dating of particulate organic matter in "dirty" speleothems (as well as other carbonates such as tufa) provides an age which is not overly distorted by contamination, but likely to be offset by 300-1000 years older than the true age of carbonate formation. The T-AQ samples (excluding T-AQ 7) define a growth period of around 400 years, which corresponds in length to the known available time-period of formation, although this is primarily driven by the younger age of T-AQ-1, with the older samples being well within error of each other. The precise degree of age offset in any particular sample will be controlled by a number of factors including the ages and leachability of the organic matter pools at the source, type of detrital input, the flow-rate and length of water transport pathways, and microbial communities present in the growth area at the time of deposition. Analysis of mineral fabrics in a sample prior to dating may help resolve some of these issues, for example via identification of micrite layers associated with low flow regimes and microbial activity.

This experiment focused on only one of the available organic fractions that can be recovered from speleothems, sinters and non-photic tufas – the humic non-acid soluble and

particulate material. It is possible that other organic matter fractions preserved may provide more accurate dates due to more rapid deposition; for example *n*-alkanes preserved in a speleothem have previously been shown to respond rapidly to changes in the overlying land-use and vegetation where other parts of the organic matter pool did not (Blyth et al., 2007). Recovery of molecules connected to specific sources such as plant derived lignins is also possible (Blyth & Watson, 2009). Aside from the issue of sample chronology, the application of radiocarbon dating to a range of organic matter fractions, might provide crucial information about the ages and transport lags associated with different parts of the organic matter signal in underground archives, and so advance our understanding of related palaeo-proxies.

## Conclusion

These results indicate that radiocarbon dating of the organic matter component in speleothems has potential for use in palaeoenvironmental sciences, but that careful choice of sample, prior analysis of mineral fabric, and isolation of the most appropriate organic matter fraction will be required. In terms of use in dating “dirty” speleothems, dating of particulate organic matter has been shown to provide an approximate indication of broad age, which may be of value as a sample screening technique and can complement what is possible by U-Th for such samples. However, a time-series dating strategy looks unlikely to be achieved with this technique alone, with feasibility depending on the origin and relative age of the particulate organic matter at the time of deposition. Further research is now required to establish the extent to which dating of other organic matter classes preserved in speleothems and tufa can contribute to chronological studies.

**Acknowledgements**

This work was supported by Australian Institute of Nuclear Science and Engineering (AINSE) Research Award ALNGRA13001, and an AINSE Research Fellowship to AJB. The Trento aqueduct flowstone sample was collected by AB and SF under permission from "Soprintintendenza per i beni culturali, Ufficio Beni Archeologici" of the Autonomous Province of Trento. The dripstone sample from Lilly-Pilly Cave was collected by Nicholas White from a manmade structure under permission from Dale Calnin, then Manager for Buchan Caves Reserve.

**References**

Adolphe, J.P. 1973, Contribution à l'etude des encroutements carbonatés de l'Aqueduc du Pont du Gard. Comptes Rendus Academie Sciences, Paris, série D, 277, p. 2329-2332.

Arenas, C., Osácar, C., Sancho, C., Vázquez-Urbez, M., Auqué, L., Pardo, G. 2010. Seasonal record from recent fluvial tufa deposits (Monasterio de Piedra, NE Spain): sedimentological and stable isotope data. Geological Society, London, Special Publication 336, 119-142.

Baker, A., Mockler, N.J., Barnes, W.L. 1999. Fluorescence intensity variations of speleothem-forming groundwaters: implications for palaeoclimate reconstruction. Water Resources Research 35, 407-413.

Baker, A., Jex, C.N., Rutlidge, H., Woltering, M., Blyth, A.J., Andersen, M.S., Cuthbert, M.O., Marjo, C.E., Markowska, M., Rau, G.C., Khan, S.J. 2016. An irrigation experiment to compare soil, water and speleothem tetraether membrane lipid distributions. Organic Geochemistry 94, 12-20.

372 Bassi, C. 2004. L'acqua e la città romana : il caso Tridentum : il fiume, i fossati, i pozzi, le
373 condutture. In: DE VOS M. (edit.), Archeologia del territorio : metodi, materiali, prospettive.
374 Medjerda e Adige : due territori a confronto. Trento, Università di Trento. Dipartimento di
375 scienze filologiche e storiche, 2004: 405-428.
376 Bassi, C. 2007. Nuovi dati sulla fondazione e l'impianto urbano di Tridentum. In: Brecciaroli
377 Tabarelli L. (edit.), Forme e tempi di urbanizzazione della Cisalpina (II secolo aC-I secolo dC)
378 – Atti delle giornate di studio. All'Insegna del Giglio, Firenze 2007: 51-59.
379 Beck, J.W., Richards, D.A., Edwards, R.L., Silverman, B.W., Smart, P.L., Donahue, D.J.,
380 Hererra-Osterheld, S., Burr, G.S., Calsoyas, L., Jull, A.J.T., Biddulph, D., 2001. Extremely large
381 variations of atmospheric $^{14}C$ concentration during the last glacial period. Science 292, 2453-
382 2458.
383 Blyth, A.J., Frisia, S. 2008. Molecular evidence for bacterial mediation of calcite formation
384 in cold high-altitude caves. Geomicrobiology Journal, 25(2), 101-111.
385 Blyth, A.J., Watson, J.S., 2009. Thermochemolysis of organic matter preserved in
386 stalagmites: a preliminary study. Organic Geochemistry, 40, 1029-1031.
387 Blyth, A.J., Farrimond, P. & Jones, M. 2006. An optimised method for the extraction and
388 analysis of lipid biomarkers from stalagmites. Organic Geochemistry, 37, 882-890.
389 Blyth, A.J., Asrat, A., Baker, A., Gulliver, P., Leng, M., Genty, D. 2007. A new approach to
390 detecting vegetation and land-use change: high resolution lipid biomarker records in
391 stalagmites. Quaternary Research 68, 314-324.
392 Blyth, A.J., Baker, A., Penkman, K.E.H., Collins, M.J., Gilmour, M.A., Moss, J.S., Genty, D. &
393 Drysdale, R. 2008. Molecular organic matter in speleothems as an environmental proxy.
394 Quaternary Science Reviews, 27, 905-921

Blyth, A.J., Shutova, Y., Smith, C.I. 2013. $\delta^{13}C$ analysis of bulk organic matter in speleothems using liquid chromatography–isotope ratio mass spectrometry. Organic Geochemistry, 55, 22-25.

Blyth, A.J., Jex, C.N., Baker, A., Khan, S., Schouten, S. 2014. Contrasting distributions of glycerol dialkyl glycerol tetraethers (GDGTs) in speleothems and associated soils. Organic Geochemistry 69, 1-10

Blyth, A.J., Fuentes, D., George, S.C., Volk, H. 2015. Characterisation of organic inclusions in stalagmites using laser-ablation-micropyrolysis gas chromatography-mass spectrometry. Journal of Analytical and Applied Pyrolysis 113, 454-463.

Blyth, A.J., Hartland, A., Baker, A. 2016. Organic proxies in speleothems – New developments, advantages and limitations. Quaternary Science Reviews 149, 1-17.

Borsato A, Frisia S, Jones B, van der Borg K. 2000. Calcite moonmilk: crystal morphology and environment of formation in caves in the Italian Alps. Journal of Sedimentary Research 70, 1179–1190.

Borsato, A., Frisia, S., Miorandi, R., van der Borg, K., Spötl, C., Corradini, F., 2007. Ricostruzioni climatico-ambientali per l'Olocene da tufo calcareo e latte di monte in grotte del Trentino. [Holocene climate and environmental reconstruction from calcareous tufa and moonmilk deposits in Trentino caves]. Studi Trent. Sci. Nat., Acta Geol 82, 239-259.

Borsato, A., Frisia, S., Miorandi, R. 2015. Carbon dioxide concentration in temperate climate caves and parent soils over an altitudinal gradient and its influence on speleothem growth and fabrics. Earth Surface Processes and Landforms 40, 1158 – 1170.

Brasier, A.T., Andrews, J.E., Kendall, A.C. 2011. Diagenesis or dire genesis? The origin of columnar spar in tufa stromatolites of central Greece and the role of chironomid larvae. Sedimentology 58, 1283-1302.

419 Bronk Ramsey, C. 2009. Bayesian analysis of radiocarbon dates. Radiocarbon 51,
420 337-360.
421 Brown, T.A., Southon, J.R. 1997. Corrections for contamination background in AMS $^{14}C$
422 measurements. Nuclear Instruments and Methods in Physics Research B 123, 208-213.
423 Cheng, H., Edwards, R.L., Shen, C.-C., Polyak, V.J., Asmerom, Y., Woodhead, J.D., Hellstrom,
424 J., Wang, Y., Kong, X., Spötl, C., Wang, X., Calvin Alexander, E., Jr, 2013. Improvements in
425 $^{230}Th$ dating, $^{230}Th$ and $^{234}U$ half-life values, and U–Th isotopic measurements by multi-
426 collector inductively coupled plasma mass spectrometry. Earth and Planetary Science
427 Letters 371–372, 82–91.
428 Donahue, D.J., Linick, T.W., Jull, A.J.T. 1990. Isotope-ratio and background corrections for
429 accelerator mass spectrometry radiocarbon measurements. Radiocarbon 32, 135-142.
430 Dorale, J.A., Edwards, R.L., Alexander Jr, E.C., Shen, C-C., Richards, D.A., Cheng, H. 2004.
431 Uranium-series dating of speleothems: current techniques, limits, and applications. In
432 Sasowsky, I.D., Mylroie, J. Studies of Cave Sediments, Springer US. 177-197.
433 Drysdale, R.N., Paul, B.T., Hellstrom, J., Couchoud, I., Greig, A., Bajo, P., Zanchetta, G., Isola,
434 I., Spötl, C., Baneschi, I., Regattieri, E., Woodhead, J.D., 2012. Precise microsampling of
435 poorly laminated speleothems for U-series dating. Quaternary Geochronology 14, 38–47.
436 Fink, D., Hotchkis, M., Hua, Q., Jacobsen, G., Smith, A.M., Zoppi, U., Child, D., Mifsud, C., van
437 der Gaast, H., Williams, A., Williams, M. 2004. The ANTARES AMS Facility at ANSTO. Nuclear
438 Instruments and Methods in Physics Research B 223-224, 109-115.
439 Frisia, S., 2015. Microstratigraphic logging of calcite fabrics in speleothems as tool for
440 palaeoclimate studies. International Journal of Speleology, 44, 1-16.
441 Frisia, S., Borsato, A., 2010. Karst. In: Alonso-Zarza, A.M. & Tanner L.H., (edit.). Development
442 in sedimentology, 61: Carbonates in continental settings: 269-315.

443 Frisia, S., Borsato, A., Fairchild, I.J., McDermott, F. 2000. Calcite fabrics, growth mechanisms,
444 and environments of formation in speleothems from the Italian Alps and Southwestern
445 Ireland. Journal of Sedimentary Research 70, 1183-1196.
446 Genty, D. 1992. Godarville tunnel speleothems (Belgium). An exceptional example of
447 modern calcite deposits. Importance for the study of the kinetics of calcite precipitation and
448 its relation to environmental variations." Speleochronos (Fac. Polyt. Mons, Belgium) 4, 3-6.
449 Genty, D., Massault, M. 1997. Bomb 14C recorded in laminated speleothems: calculation of
450 dead carbon proportion. Radiocarbon 39, 33-48.
451 Genty, D., Massault, M., 1999. Carbon transfer dynamics from bomb-14C and d13C time
452 series of a laminated stalagmite from SW France e modelling and comparison with other
453 stalagmite records. Geochimica et Cosmochimica Acta 63, 1537-1548.
454 Genty, D., Baker, A., Massault, M., Proctor, C., Gilmour, M., Pons-Branchu, E., Hamelin, B.,
455 2001. Dead carbon in stalagmites: carbonate bedrock palaeodissolution vs. ageing of soil
456 organic matter. Implications for $^{13}C$ variations in speleothems. Geochimica et Cosmochimica
457 Acta 65, 3443-3457.
458 Genty, D., Konik, S., Valladas, H., Blamart, D., Hellstrom, J., Touma, M., Moreau, C.,
459 Dumoulin, J-P., Nouet, J., Duaphin, Y., Weil, R. 2011. Dating the Lascaux Cave Gour
460 Formation. Radiocarbon 53, 479-500.
461 Gradziński, M. 2010. Factors controlling growth of modern tufa: results of a field
462 experiment. Geological Society, London. Special Publications 336, 143-191.
463 Griffiths, M.L., Fohlmeister, J., Drysdale, R.N., Hua, Q., Johnson, K.R., Hellstrom, J.C., Gagan,
464 M.K., Zhao, J.-x., 2012. Hydrological control on the dead-carbon content of a tropical
465 Holocene speleothem. Quaternary Geochronology 14, 81-93.

466 Guendon, J.L., & Vaudour, J. 1986. Les concrétions de l'aqueduc de Nimes, observations et
467 hypothèses. Mediterranée, 1-2, p.140-151.
468 Hellstrom, J., 2003. Rapid and accurate U/Th dating using parallel ion-counting multi-
469 collector ICP-MS. Journal of Analytical Atomic Spectrometry 18, 1346–1351.
470 Hellstrom, J. 2006. U-Th dating of speleothems with high initial $^{230}$Th using stratigraphical
471 constraint. Quaternary Geochronology 1, 289-295.
472 Hellstrom, J., Pickering, R., 2015. Recent advances and future prospects of the U–Th and U–
473 Pb chronometers applicable to archaeology. Journal of Archaeological Science 56, 32–40.
474 Hobley, E., Willgoose, G., Frisia, S., Jacobsen, G., 2014. Stability and storage of soil organic
475 carbon in a heavy-textured karst soil from south-eastern Australia. Soil Research 52, 476-
476 482
477 Hodge, E., McDonald, J., Fischer, M., Redwood, D., Hua, Q., Levchenko, V., Drysdale, R.,
478 Waring, C., Fink, D. 2011. Using the $^{14}$C bomb pulse to date young speleothems.
479 Radiocarbon 53, 345-357.
480 Hoffman, D.L., Beck, J.W., Richards, D.A., Smart, P.L., Singarayer, J.S., Ketchmark, T.,
481 Hawkesworth, C.J. 2010. Towards radiocarbon calibration beyond 28 ka using speleothems
482 from the Bahamas. Earth and Planetary Science Letters 289, 1-10.
483 Hogg, A.G., Hua, Q., Blackwell, P.G., Niu, M., Buck, C.E., Guilderson, T.P., Heaton, T.J.,
484 Palmer, J.G., Reimer, P.J., Reimer, R.W., Turney, C.S.M., Zimmerman, S.R.H. 2013. SHCal13
485 Southern Hemisphere calibration, 0-50,000 cal yr BP. Radiocarbon 55, 1889-1903.
486 Hua, Q., Jacobsen, G.E., Zoppi, U., Lawson, E.M., Williams, A.A., Smith, A.M., McGann, M.J.
487 2001. Progress in radiocarbon target preparation at the ANTARES AMS Centre. Radiocarbon
488 43, 275-282.

Hua, Q., Zoppi, U., Williams, A.A., Smith, A.M. 2004. Small-mass radiocarbon analysis at ANTARES. Nuclear Instruments and Methods in Physics Research B 223-224, 284-292.

Hua, Q., McDonald, J., Redwood, D., Drysdale, R., Lee, S., Fallon, S., Hellstrom, J. 2012. Robust chronological reconstruction for young speleothems using radiocarbon. Quaternary Geochronology 14, 67-80.

Labonne, M., Hillaire_Marcel, C., Ghaleb, B., Goy, J-L. 2002. Multi-isotopic age assessment of dirty speleothem calcite: an example from Altamira Cave, Spain. Quaternary Science Reviews 21, 1099-1110.

Li, X., Hi, C., Huang, J., Xie, S., Baker, A. 2014. A 9000-year carbon isotopic record of acid-soluble organic matter in a stalagmite from Heshang Cave, central China: Palaeoclimate implications. Chemical Geology 388, 71-77.

Meyer, M.C., Spötl, C., Mangini, A., Tessadri, R. 2012. Speleothem deposition at the glaciation threshold – An attempt to constrain the age and palaeoenvironmental significance of a detrital-rich flowstone sequence from Entrische Kirche Cave (Austria). Palaeogeography, Palaeoclimatology, Palaeoecology 319-320, 93-106.

Noronha, A.L., Johnson, K.R., Hu, C., Ruan, J., Southon, J.R., Ferguson, J.E., 2014. Assessing influences on speleothem dead carbon variability over the Holocene: Implications for speleothem-based radiocarbon calibration. Earth Planetary Science Letters 394, 20-29.

Özkul, M., Gökgöz, A., Horvantinčić, N. 2010. Depositional properties and geochemistry of Holocene perched springline tufa deposits and associated spring waters: a case study from the Denizli Province, Western Turkey. Geological Society, London, Special Publications 336, 245-262.

Pelczar Jr, M. J., Reid, R. D., Chan, E. C. S. 1982. Cultivation of bacteria. Tata McGraw Hill Publishing Co. Ltd., New Delhi 103pp.

513 Quiers, M., Perrette, Y., Chalmin, E., Fanget, B. and Poulenard, J. 2015. Geochemical
514 mapping of organic carbon in stalagmites using liquid-phase and solid-phase fluorescence.
515 Chemical Geology 411, 240-247.
516 Reimer, P.J., Bard, E., Bayliss, A., Beck, J.W., Blackwell, P.G., Bronk Ramsey, C., Buck, C.E.,
517 Cheng, H., Edwards, R.L., Friedrich, M., Grootes, P.M., Guilderson, T.P., Hafl-idason, H.,
518 Hajdas, I., Hatté, C., Heaton, T.J., Hoffmann, D.L., Hogg, A.G., Hughen, K.A., Kaiser, K.F.,
519 Kromer, B., Manning, S.W., Niu, M., Reimer, R.W., Richards, D.A., Scott, E.M., Southon, J.R.,
520 Staff, R.A., Turney, C.S.M., van der Plicht, J. 2013. IntCal13 and Marine13 radiocarbon age
521 calibration curves 0–50,000 years cal BP. Radiocarbon55, 1869-1887.
522 Richards, D., Dorale, J., 2003. Uranium-series chronology and environmental applications of
523 speleothems. Reviews in Mineralogy and Geochemistry 52, 407-460.
524 Rogerson, M., Pedley, H.M., Wadhawan, J.D., Middleton, R. 2008. New insights into
525 biological influence on the geochemistry of freshwater carbonate deposits. Geochimica et
526 Cosmochimica Acta 72, 4976-4987.
527 Rudzka, D., McDermott, F., Baldini, L.M., Fleitmann, D., Moreno, A., Stoll, H., 2011. The
528 coupled $\delta^{13}$C-radiocarbon systematics of three Late Glacial/early Holocene speleothems;
529 insights into soil and cave processes at climatic transitions. Geochimica et Cosmochimica
530 Acta 75, 4321-4339.
531 Scholz, D., Frisia, S., Borsato, A., Spötl, C., Fohlmeister, J., Mudelsee, M., Miorandi, R.,
532 Mangini, A., 2012. Holocene climate variability in north-eastern Italy: potential influence of
533 the NAO and solar activity recorded by speleothem data. Climate of the Past 8, 1367-1383.
534 Southon, J., Noronha, A.L., Cheng, H., Edwards, R.L., Wang, Y. 2012. A high-resolution record
535 of atmospheric $^{14}$C based on Hulu Cave speleothem H82. Quaternary Science Reviews 33,
536 32-41.

Van Beyen, P., Bourbonniere, R., Ford, D., Schwarcz, H. 2001. Causes of colour and fluorescence in speleothems. Chemical Geology 175, 319–34.

Woodhead, J., Hellstrom, J., Maas, R., Drysdale, R., Zanchetta, G., Devine, P., Taylor, E. 2006. U-Pb geochronlogy of speleothems by MC-ICPMS. Quaternary Geochronology, 1, 208-221.

**Table and figure captions**

**Table 1.** U-Th data for the top (Aq.T) and base (Aq.B) of the T-AQ flowstone sinter

**Table 2** - Radiocarbon results of particulate samples extracted from LP and T-AQ speleothems. Note: Calendar age conversion was performed using OxCal Program v.4.2 (Bronk Ramsey, 2009), and the SHCal13 data set (Hogg et al., 2013) for LP samples or the IntCal13 Data set (Reimer et al., 2013) for T-AQ samples.

**Figure 1.** T-AQ thin section showing sparry columnar calcite crystals capped by micrite peloids. The micrite layer incorporates small bivalves. Note that crystal splitting occurs toward the top of columnar crystals, most probably coinciding with the input of organic compounds. These likely facilitated the occurrence of micrite. The bottom edge of the photo is 7 mm across.

**Figure 2.** Subsection of the T-AQ flowstone sample showing the eight groups of layers sampled. Note the clear detrital layers associated with level 7.

**Figure 3.** Measured pMC vs carbon mass for lignin alkaline (A) and powdered graphite (B). Lines denote hyperbolic curves in the form of pMC = a + b/Mass fitted to the experimental data (solid dots), with a and b being constant and subscripts la and g designating for lignin alkali and graphite, respectively. Error bars are 1σ.

560 **Figure 4.** The T-AQ age data. Black dots are median calibrated 14C ages, with error bars
561 showing the 95.4% probability age ranges. Black crosses are the top and basal U-Th dates,
562 which show an age inversion. The green/grey box shows the archaeological age of formation
563 of the flowstone.

564

| Sample | U(ngg$^{-1}$) | [$^{230}$Th/$^{238}$U]$^{a}$ | [$^{234}$U/$^{238}$U]$^{a}$ | [$^{232}$Th/$^{238}$U] | [$^{230}$Th/$^{232}$Th] | Age(ka BP)$^{b}$ | [$^{234}$U/$^{238}$U]$_{i}^{c}$ |
|---|---|---|---|---|---|---|---|
| Aq.T | 95 | 0.1242(34) | 1.3740(28) | 0.1075(23) | 1.16 | 1.9(0.6) | 1.3761(29) |
| Aq.B | 144 | 0.0946(63) | 1.3724(39) | 0.08175(26) | 1.16 | 1.4(0.6) | 1.3740(40) |

[a] Activity ratios determined after Hellstrom (2003) and Drysdale et al (2012)

[b] Age in kyr before 1950 AD corrected for intial $^{230}$Th using eqn. 1 of Hellstrom (2006), the decay constants of Cheng et al (2013) and [230Th/232Th]i of 0.94 ± 0.05

[c] Initial [$^{234}$U/$^{238}$U] calculated using corrected age

2-σ uncertainties in brackets are of the last two significant figures presented

Table 1. U-Th data for the top (Aq.T) and base (Aq.B) of the T-AQ flowstone sinter

| Sample ID | Lab ID | $\delta^{13}C$ (‰) | Sample Mass (mgC) | | Measured pMC | | Blank-corrected pMC | | Conv. $^{14}C$ Age (BP) | | Calibrated $^{14}C$ Age (cal years BP) | | | | |
|---|---|---|---|---|---|---|---|---|---|---|---|---|---|---|---|
| | | | Mean | 1σ | Mean | 1σ | Mean | 1σ | Mean | 1σ | 68.2% probability | | 95.4% probability | | Median |
| LP13 r1 | OZR099 | -20.7 | 0.1037 | 0.0011 | 92.98 | 0.35 | 95.86 | 0.48 | 340 | 40 | | | | | |
| LP13 | OZR100 | -20.7 | 0.0879 | 0.0010 | 93.38 | 0.36 | 96.80 | 0.53 | 261 | 44 | | | | | |
| LP13 mean | | | | | | | | | 304 | 55 | 446 | 158 | 486 | 148 | 336 |
| T-AQ-1 | OZR101 | -24.5 | 0.1759 | 0.0100 | 74.48 | 0.32 | 75.74 | 0.35 | 2232 | 38 | 2322 | 2160 | 2337 | 2153 | 2232 |
| T-AQ-2 | OZR102 | -23.6 | 0.1859 | 0.0100 | 72.47 | 0.57 | 73.63 | 0.59 | 2460 | 64 | | | | | |
| T-AQ-2r | OZR103 | -24.5 | 0.1191 | 0.0013 | 70.95 | 0.41 | 72.69 | 0.46 | 2562 | 51 | | | | | |
| T-AQ-2 mean | | | | | | | | | 2522 | 71 | 2745 | 2492 | 2753 | 2380 | 2587 |
| T-AQ-3 | OZR104 | -24.5 | 0.1443 | 0.0015 | 72.58 | 0.35 | 74.06 | 0.39 | 2412 | 43 | | | | | |
| T-AQ-3r | OZR105 | -24.5 | 0.0822 | 0.0009 | 70.76 | 0.35 | 73.28 | 0.46 | 2498 | 51 | | | | | |
| T-AQ-3 mean | | | | | | | | | 2447 | 60 | 2697 | 2365 | 2714 | 2357 | 2532 |
| T-AQ-4 | OZR106 | -25.4 | 0.1283 | 0.0014 | 72.26 | 0.34 | 73.92 | 0.39 | 2428 | 43 | 2680 | 2360 | 2704 | 2353 | 2481 |
| T-AQ-5 | OZR107 | -23.0 | 0.1659 | 0.0100 | 72.04 | 0.41 | 73.32 | 0.44 | 2493 | 48 | | | | | |
| T-AQ-5r | OZR108 | -25.3 | 0.1659 | 0.0100 | 71.64 | 0.27 | 72.91 | 0.31 | 2538 | 34 | | | | | |
| T-AQ-5 mean | | | | | | | | | 2523 | 30 | 2737 | 2514 | 2745 | 2492 | 2599 |
| T-AQ-6 | OZR109 | -24.3 | 0.1440 | 0.0015 | 73.03 | 0.32 | 74.53 | 0.37 | 2361 | 40 | | | | | |
| T-AQ-6r | OZR110 | -25.3 | 0.1659 | 0.0100 | 72.61 | 0.33 | 73.90 | 0.36 | 2430 | 40 | | | | | |
| T-AQ-6 mean | | | | | | | | | 2395 | 48 | 2651 | 2350 | 2701 | 2340 | 2444 |
| T-AQ-7 | OZR111 | -24.5 | 0.0590 | 0.0008 | 69.47 | 0.59 | 72.88 | 0.72 | 2541 | 80 | | | | | |
| T-AQ-7r | OZR112 | -24.5 | 0.0825 | 0.0009 | 67.54 | 0.47 | 69.89 | 0.55 | 2878 | 64 | | | | | |
| T-AQ-7 mean | | | | | | | | | 2747 | 232 | 3211 | 2508 | 3449 | 2342 | 2889 |
| T-AQ-8 | OZR113 | -24.5 | 0.0613 | 0.0008 | 70.34 | 0.42 | 73.68 | 0.59 | 2453 | 64 | 2700 | 2380 | 2717 | 2358 | 2539 |

Table 2 - Radiocarbon results of particulate samples extracted from LP and T-AQ speleothems

Note: Calendar age conversion was performed using OxCal Program v.4.2 (Bronk Ramsey, 2009), and the SHCal13 data set (Hogg et al., 2013) for LP samples or the IntCal13 Data set (Reimer et al., 2013) for T-AQ samples.

Figure 1.

Figure 2.

Figure 3.

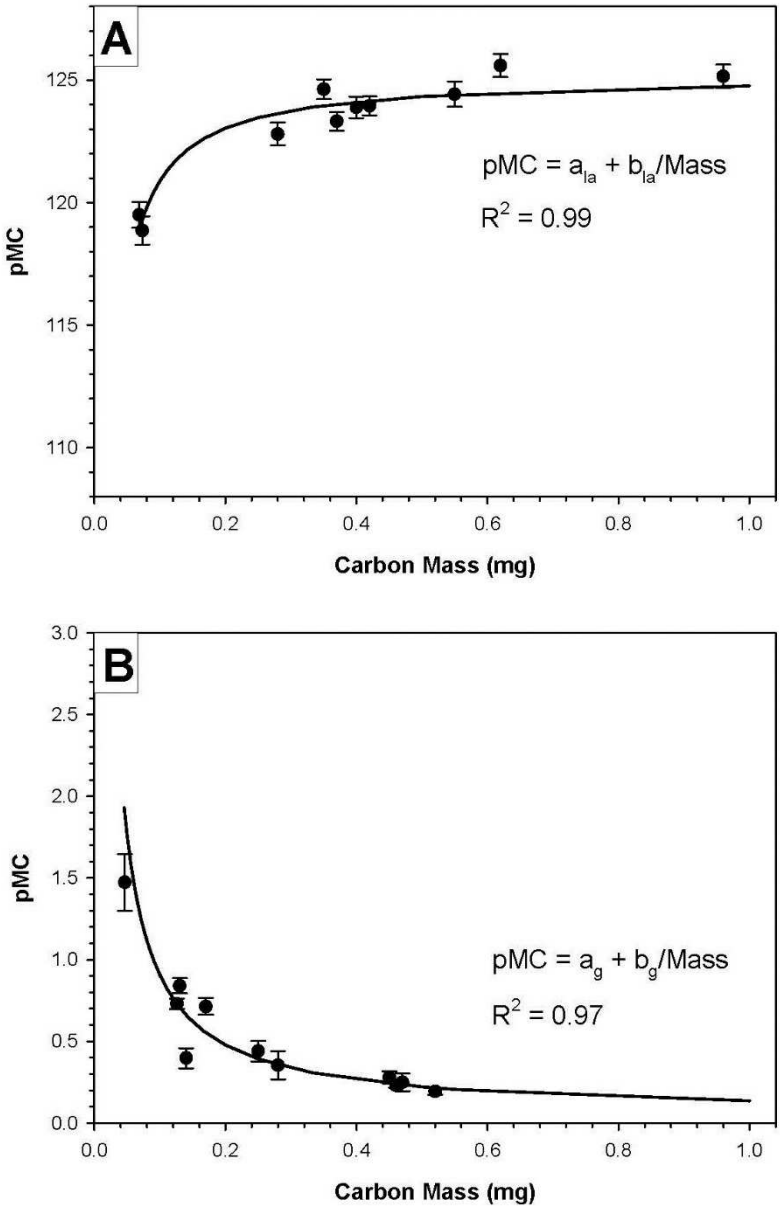
A
pMC = $a_{la}$ + $b_{la}$/Mass
$R^2$ = 0.99
pMC
Carbon Mass (mg)
B
pMC = $a_g$ + $b_g$/Mass
$R^2$ = 0.97
pMC
Carbon Mass (mg)

Figure 4.

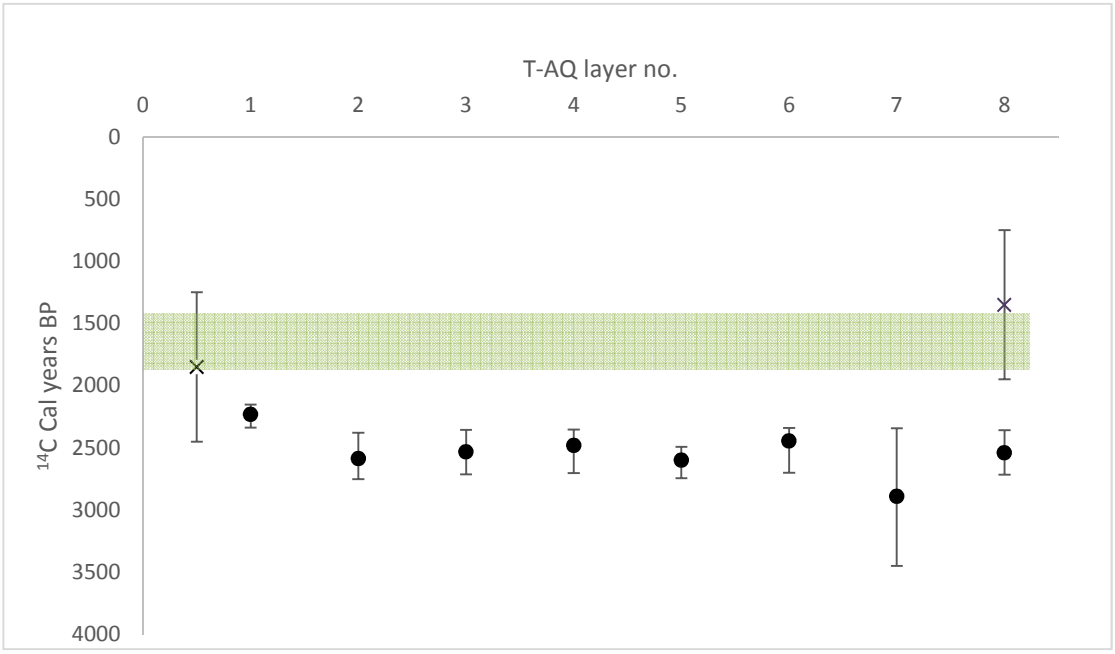
T-AQ layer no.
0
1
2
3
4
5
6
7
8
0
500
1000
1500
2000
2500
3000
3500
4000
14C Cal years BP

Highlights

- Speleothems contain particulate and non-acid soluble organic matter amenable to radiocarbon dating
- Dates from the OM are consistently 300 – 1000 years older than the known date of formation
- The offset is hypothesised to derive from transported and reworked organic carbon